Chemical Science

ROYAL SOCIETY OF CHEMISTRY

EDGE ARTICLE

View Article Online
View Journal | View Issue

Cite this: *Chem. Sci.*, 2025, **16**, 10867

All publication charges for this article have been paid for by the Royal Society of Chemistry

Received 24th February 2025
Accepted 8th May 2025

DOI: 10.1039/d5sc01474c

rsc.li/chemical-science

A conformationally adaptable tetrahedral cage with different guest encapsulation models†

Hua Tang,[a] Yuyang Lu,[a] Yongwei Qian,[a] Chenqi Ge,[a] Jiyong Liu,[a] Hongliang Chen *[ab] and Hao Li *[ab]

Through imine condensation, a tetrahedral cage-shaped molecule was obtained in a one-pot manner, which comprises four trisamino vertices and four trisformyl faces each containing three *meta*-methyl-pyridyl units. Within the cage framework, each of the twelve pyridines undergoes pivoting around the corresponding imine-pyridine-phenyl axle, endowing the cage with adaptable conformations. By modulating the number of pyridyl nitrogen atoms that point inwards, the cage can switch the effective volume of its cavity where a wide range of guest molecules including quaternary ammoniums, or different amounts of alkali cations, are encapsulated, by utilizing dipole–cation forces and/or hydrogen bonding. This behavior is reminiscent of biological enzymes that can adjust their conformations to optimize binding affinity.

Introduction

Biological acceptors can precisely modulate their conformations to optimize their binding affinity towards target substrates.[1] A typical example of adapting conformations in regulation of guest upload and release is hemoglobin.[2] This enzyme cooperatively accommodates four oxygen molecules in one conformation and switches to another that favors the release of all oxygens. This behavior enhances the ability of hemoglobin to deliver oxygen. In order to unravel the underlying mechanism of how these conformational change behaviors occur, one of the often-used approaches is to synthesize artificial hosts, whose conformations can be modulated precisely with different guest binding models.[3] Various metal–ligand coordinative macrocycles[4,5] and cages[6–12] have been developed for this purpose. Their conformations can be adjusted upon recognition of different guests, and in some cases, multiple guests could be recognized within the host cavities in either a positive[13–16] or negative[17,18] cooperative manner. As a comparison, using purely covalent hosts[19–24] to achieve conformationally adaptive guest binding has been much less successful. Purely covalent hosts self-assembled *via* dynamic covalent chemistry[25–30] often comprise relatively rigid building blocks, in order to suppress entropy loss in self-assembly for the sake of high yields. The rigidity, on the other hand, would jeopardize the adaptability of conformations. Examples[31,32] of purely covalent cages, which can incorporate the advantages of both high yielding synthesis and adaptability of conformation with different binding modes, are still rare.

Here, we obtained a tetrahedral molecule in high yield (*i.e.*, 88%), by condensing four equivalents of trisamine as vertices and four trisformyl residues as faces each bearing three *meta*-methyl-pyridyl units. The relatively high yield of the cage results from intramolecular forces including CH···π interactions. Within the cage framework, each of the twelve *meta*-methyl-pyridyl units undergoes free pivoting motion around the corresponding imine-pyridyl-phenyl axle, allowing the cage to adopt different conformations. In the absence of guests, on average, six of the twelve pyridyl nitrogen atoms point inwards while the others point out, implying that the "free" cage cavity is occupied by six methyl units. The cage can adapt its conformation to recognize a wide range of guests, by switching or decreasing the number of methyl units that are located inside the cavity. The pyridyl units afford the cage the ability to recognize Lewis acidic guests including quaternary ammoniums and alkali cations, by providing hydrogen bonding and/or cation–dipole interactions. For example, by adopting a conformation with nine pyridyl nitrogen atoms pointing inwards, the cage can encapsulate a single Na^+ cation. When all twelve pyridyl nitrogen atoms are directed inward, the cage can accommodate two cations simultaneously.

Results and discussion

The triangular trisformyl compound **F1** was synthesized *via* Suzuki coupling. In **F1**, each of the formyl units is grafted at the 5-position of a *meta*-methyl-pyridyl unit. **F1** was combined with

[a]*Stoddart Institute of Molecular Science, Department of Chemistry, Zhejiang University, Hangzhou 310058, China. E-mail: lihao2015@zju.edu.cn; hongliang.chen@zju.edu.cn*

[b]*Zhejiang-Israel Joint Laboratory of Self-Assembling Functional Materials, ZJU-Hangzhou Global Scientific and Technological Innovation Center, Zhejiang University, Hangzhou 311215, China*

† Electronic supplementary information (ESI) available. CCDC 2395426, 2396911 and 2441591. For ESI and crystallographic data in CIF or other electronic format see DOI: https://doi.org/10.1039/d5sc01474c

tris(2-aminoethyl)amine (TREN), a commercially available trisamine, in $CDCl_3$. After placing the solution at room temperature for 30 h, the recorded ^{1}H NMR spectrum revealed a new set of sharp resonances corresponding to a tetrahedral cage **T1** (Fig. 1 and S14, ESI†). This tetrahedron is composed of four TREN residues as the vertices and four **F1** residues as the faces. The self-assembly yield of **T1** was determined to be 88%, by integrating and comparing the resonances corresponding to the formyl precursor **F1** and the product **T1** relative to an internal standard in the NMR sample, whose concentration remained constant before and after self-assembly (Fig. S14, ESI†). Such a high yield of **T1** resulted from the dynamic nature of imine formation, during which error checking was allowed so that the system was able to search for its thermodynamic minimum. A pure solid-state sample of **T1** was isolated in 57% yield *via* crystallization by diffusion of isopropyl ether into its chloroform solution. This solid was then re-dissolved in $CDCl_3$ for the ^{1}H NMR spectrum, in which **T1** was the only observable product, indicating that no decomposition occurred during isolation. The formation of **T1** was further confirmed by mass spectrometry (Fig. S13, ESI†) and ^{1}H-DOSY NMR spectroscopy (Fig. S12, ESI†).

As a comparison, **F2**, an analogue of **F1** whose Me units are replaced with protons, was also combined with TREN under the same conditions. However, the formation of the putative tetrahedral cage **T2** was not observed (Fig. S16, ESI†). The self-assembly of **T2** was not successful either, even when employing quaternary ammonium species as potential templating agents. It has been reported by us[33–36] that the formation of tetrahedra was favored by the intramolecular CH···π interactions between the two adjacent phenylene units in each corner of the cage. In the case of **T1**, the occurrence of CH···π interactions requires pyridyl in each vertex to orientate in an edge-in manner. This twisted conformation indeed occurs in the precursor **F1** before self-assembly, because of the steric hindrance between the methyl units in the pyridine and the corresponding protons in the central phenyl ring. As a comparison, **F2** adopts a relatively planar conformation due to the absence of methyl units, making the formation of the putative cage **T2** more energy demanding.

The presence of CH···π interactions within the framework of **T1** was confirmed by its ^{1}H NMR spectrum (Fig. 2b). The resonances corresponding to the two protons in the *ortho* positions relative to the imine bond, denoted as protons *a* and *b*, underwent remarkable upfield shifts by 0.81 and 1.06 ppm, respectively, compared to the precursor **F1** (Fig. S3, ESI†). These shifts suggest that in the framework of **T1**, both *a* and *b* spend a substantial amount of time near the surface of an adjacent pyridyl unit, resulting in a shielded magnetic environment. Considering that only one set of sharp resonances was observed, it is thus reasonable to propose that each pyridyl underwent fast pivoting motion along the phenyl-pyridyl-imine axis on the timescale of ^{1}H NMR spectroscopy. Compared to **F1**, the resonance corresponding to the methyl unit in the cage **T1** shifted upfield by 0.52 ppm, further confirming our hypothesis

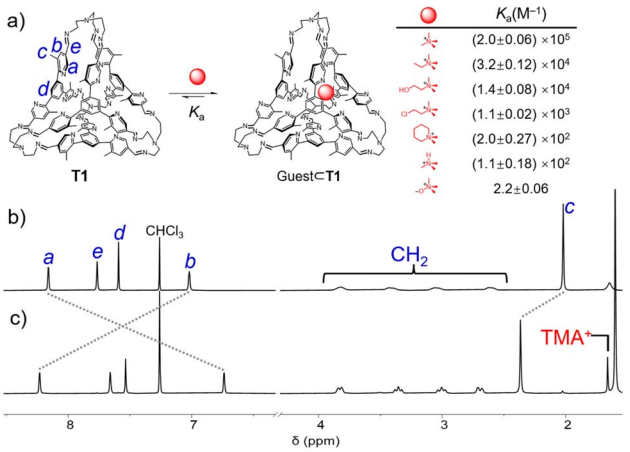

Fig. 2 (a) Recognition of a guest within the cavity of the tetrahedron **T1**. The structures of the guests and the corresponding binding constants are listed. The partial ^{1}H NMR spectrum of **T1** (400 MHz, $CDCl_3$, 298 K) (b) before and (c) after 1 equiv. of $TMA^+ \cdot Cl^-$ was added.

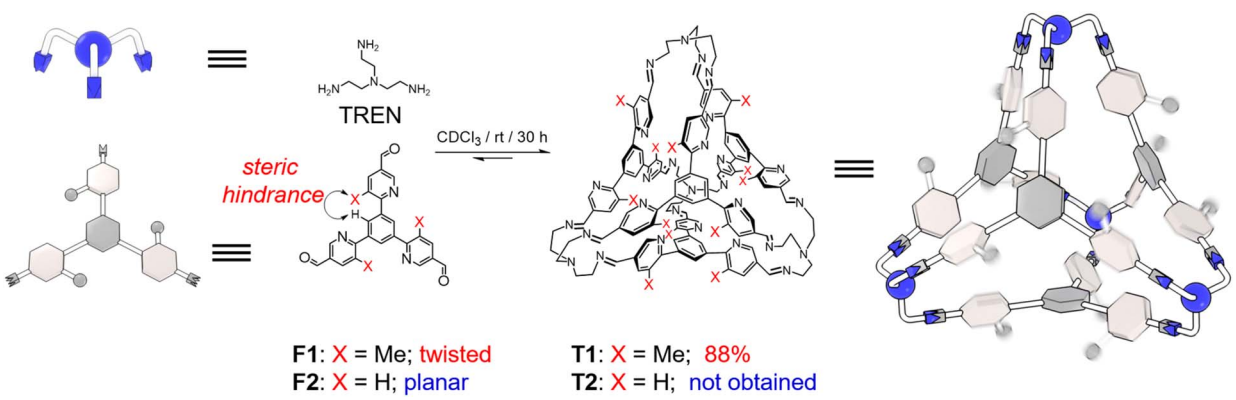

Fig. 1 Structural formula and graphic representation of a tetrahedral cage **T1** by condensing **F1** and TREN in $CDCl_3$. **F1** adopts a twisted conformation due to the steric hindrance between the methyl unit and a central phenyl proton, which proved to be of importance in the cage self-assembly. A putative tetrahedron **T2**, however, was not obtained by using an analogous formyl precursor **F2** and TREN, on account of the planar conformation of **T2**.

that the methyl units spent substantial amounts of time within the cage cavity.

The nitrogen atom in a pyridyl unit represents a typical Lewis basic binding site, endowing the cage **T1** with the ability to recognize Lewis acidic guests. Upon the addition of tetramethylammonium (TMA^+) chloride into a solution of **T1** in $CDCl_3$, the resonances of the latter underwent remarkable shifts (Fig. 2c). A resonance corresponding to TMA^+ encapsulated within the cage cavity was observed at 1.66 ppm, which shifted upfield by 1.88 ppm compared to the "free" TMA^+. This observation confirmed the recognition of TMA^+ within the cage cavity. Compared to the "free" cage **T1**, the resonance corresponding to the protons *a* in the *ortho* position of nitrogen shifted upfield by 1.42 ppm, while those corresponding to the methyl units and the protons *b* near the methyl units shifted downfield by 0.35 and 1.21 ppm, respectively. These observations clearly indicated that upon recognition of TMA^+, all the methyl units in the cage framework moved out from the cage cavity, and simultaneously all the nitrogen atoms moved inside to form cation–dipole interactions with the guest and N···HC hydrogen bonds with the methyl protons in TMA^+. The complex $TMA^+\subset$**T1**$\cdot Cl^-$ underwent slow host–guest association/dissociation exchange on the timescale of ^{1}H NMR spectroscopy, as inferred from the fact that the "free" cage and the host–guest complex exhibited two independent sets of resonances. By integrating the resonances corresponding to the "free" cage, "free" guest, and the host–guest complex, the binding constant (K_a) of $TMA^+\subset$**T1**$\cdot Cl^-$ was determined to be $(2.0 \pm 0.06) \times 10^5$ M^{-1} (Fig. S25, ESI†). Using UV-vis absorption spectroscopy, K_a was measured to be $(5.9 \pm 0.4) \times 10^4$ M^{-1} (Fig. S24, ESI†), which is in close agreement with the ^{1}H NMR spectroscopic results. We also investigated the possibility of the cage to recognize other quaternary ammonium guests. After adding tetraethylammonium (TEA^+) chloride, no changes were observed in the ^{1}H NMR spectrum of **T1**, indicating that the size of TEA^+ is too large to fit within the cavity of **T1**. In the case of trimethylethylammonium ($TMEA^+$) with I^- counterions, as well as choline, chlormequat, mepiquat and trimethylamine hydrochloride ($TMAH^+\cdot Cl^-$), whose counterions are all Cl^-, the binding constants were measured to be $(3.2 \pm 0.12) \times 10^4$ M^{-1} (Fig. S69, ESI†), $(1.4 \pm 0.08) \times 10^4$ M^{-1} (Fig. S75, ESI†), $(1.1 \pm 0.02) \times 10^3$ M^{-1} (Fig. S76, ESI†), $(2.0 \pm 0.27) \times 10^2$ M^{-1} (Fig. S89, ESI†) and $(1.1 \pm 0.18) \times 10^2$ M^{-1} (Fig. S94, ESI†), respectively. These binding constants are one or two orders of magnitude lower than that of TMA^+. One explanation is that these guests have less complementary sizes relative to the cage cavity. We also attempted to use **T1** to recognize neutral compounds with complementary sizes. However, only one zwitterion namely trimethylamine *N*-oxide was observed to be encapsulated within the cage cavity of **T1**. The binding constant was measured to be only 2.2 ± 0.06 M^{-1} by using the ^{1}H NMR spectrum (Fig. S80, ESI†), which is lower by nearly four or five orders of magnitude compared to the cationic guest TMA^+. This result indicated that the binding between **T1** and the aforementioned quaternary ammonium guests mainly relied on dipole–cation interactions.

The ability of the cage to recognize alkali cations was then investigated. Sodium tetrakis[3,5-bis(trifluoromethyl)phenyl] borate ($Na^+\cdot BArF^-$) was added into a solution of **T1** in $CDCl_3$. The $BArF^-$ counterion served to enhance the solubility of Na^+ in $CDCl_3$. Upon the addition of one equiv. of Na^+, a remarkable change occurred to the ^{1}H NMR spectrum of **T1** (Fig. 3d). The resonances corresponding to the protons *e* in imine units and protons *d* in the central phenyl units only underwent modest shifts. As a comparison, the resonances corresponding to the protons *a* and *b* in the pyridyl units were observed to broaden out into the baseline and become almost unobservable. This observation indicated that after recognition of one Na^+ cation within the cage cavity, the pivoting of pyridyl units was significantly slowed down compared to the "free" cavity, on account of cation–dipole interactions between Na^+ and pyridyl nitrogen atoms. In fact, the resonances corresponding to the protons *a* and *b* gradually sharpened at elevated temperatures. These two resonances were observed at 7.33 and 7.78 ppm, respectively at 323 K (Fig. 3c), implying an upfield and a downfield shift by 0.83 and 0.75 ppm respectively relative to the "free" cage. This observation is not surprising, because after accommodation of a Na^+ guest, more nitrogen atoms in the pyridyl units would point inwards, in order to enhance the cation–dipole interactions with the cationic guest. The ^{1}H NMR spectrum of $Na^+\subset$**T1**$\cdot BArF^-$ was also recorded at 213 K (Fig. 3e). At such a low temperature, each resonance of the cage observed at room temperature splits into four distinct peaks. For example, the resonances corresponding to the methyl units (protons *c*) were observed at 2.48, 2.45, 2.27, and 1.61 ppm respectively, while those corresponding to the protons *b* in the *ortho* positions of the methyl units were observed at 8.41, 8.38, 8.24, and 5.31 ppm, respectively. In both cases, one of the four resonances undergoes a remarkable upfield shift while the other three are located relatively downfield. The resonances corresponding to the protons *a* beside pyridyl nitrogen atoms have the opposite trend, *i.e.*, one was observed at a downfield position (*i.e.* 9.17 ppm), while the other three were located upfield (*i.e.*, 6.70, 6.68, and 6.43 ppm, respectively). Considering that the cage bears twelve pyridyl units, the appearance of four resonances indicated that the framework of the complex $Na^+\subset$**T1**$\cdot BArF^-$ has a C_3 axis of symmetry. The Na^+ guest coordinates with the three pyridyl units in one corner of the tetrahedron, driving all three methyl in this corner to reside outside the cage cavity. In each of the other three corners where the cation is absent, one methyl points inwards and occupies the cavity while the other two reside outside, driven by intramolecular Me···N hydrogen bonding. At 213 K, the motion of Na^+ between the four corners of the cage occurred at a relatively slow rate on the timescale of ^{1}H NMR spectroscopy. However, raising temperature will speed up this motion, making the four corners of the cage chemically equivalent. This proposition is consistent with the observation that at room temperature or 323 K, only one set of resonances of $Na^+\subset$**T1** was observed.

Addition of another equiv. of Na^+ into $Na^+\subset$**T1**$\cdot BArF^-$ led to the appearance of a new set of resonances in the corresponding ^{1}H NMR spectrum (Fig. 3f), corresponding to a ternary complex namely $(Na^+)_2\subset$**T1**$\cdot 2BArF^-$. Compared to $Na^+\subset$**T1**$\cdot BArF^-$, the resonances corresponding to the methyl units and protons *b* undergo downfield shifts by 0.09 and 0.62 ppm respectively,

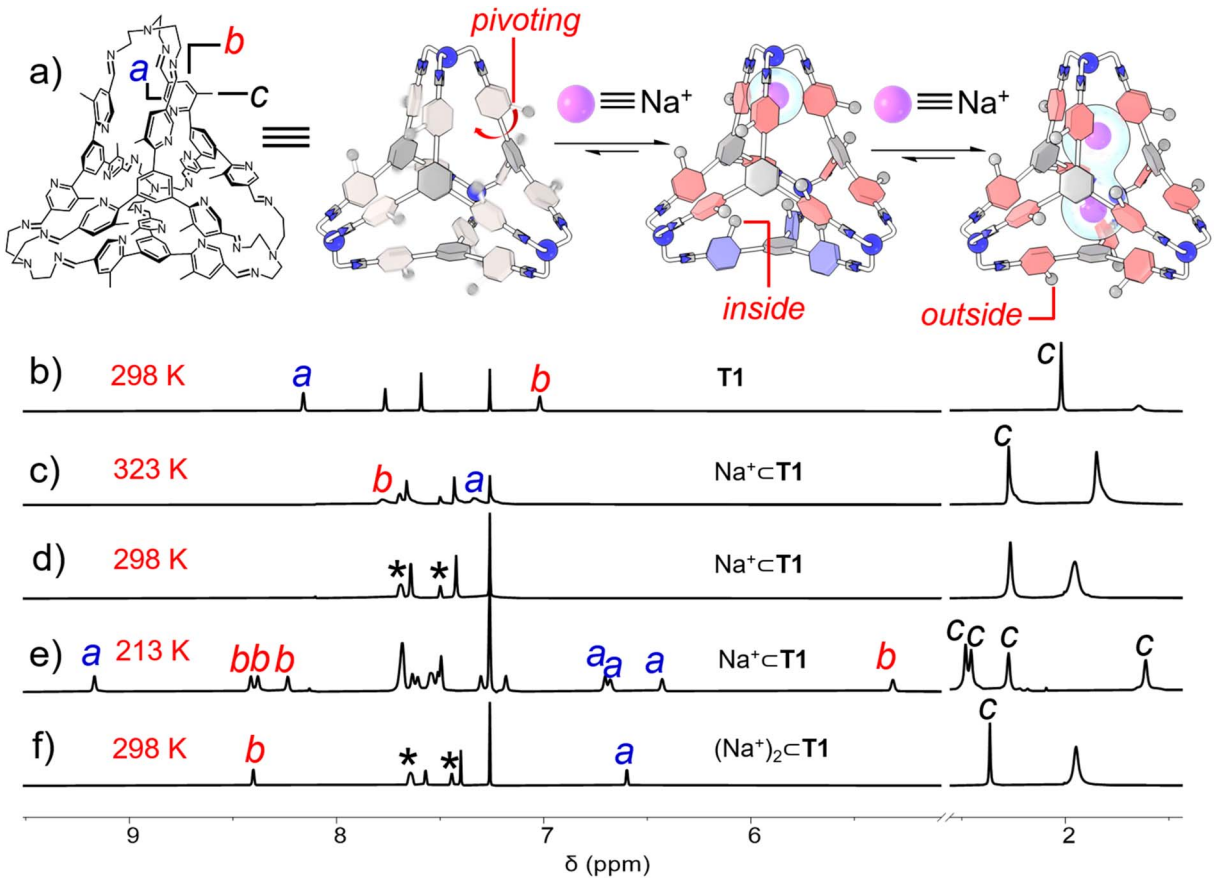

Fig. 3 (a) Graphical representation of the allosteric regulated binding behaviors of cage **T1** toward one of the two Na^+. Partial ^1H NMR spectra (400 MHz, $CDCl_3$) of (b) **T1** recorded at 298 K, $Na^+\subset$**T1**·$BArF^-$ recorded at (c) 323 K, (d) 298 K, and (e) 213 K, and (f) $(Na^+)_2\subset$**T1**·$2BArF^-$ recorded at 298 K. The resonances corresponding to the protons *a*, *b*, and *c* in the cage framework were labelled with the corresponding letters in the spectra. The resonances corresponding to the $BArF^-$ counterions were labelled with black stars.

while that of the proton *a* shifted upfield by 0.73 ppm. These shifts indicate that after the addition of the second equiv. of Na^+, all twelve pyridyl units point inward due to the occurrence of cation–dipole interactions and thus drive all twelve methyl units to reside outside the cage cavity. Unlike $Na^+\subset$**T1**·$BArF^-$ whose ^1H NMR spectrum is temperature dependent, the ^1H NMR spectrum of $(Na^+)_2\subset$**T1**·$2BArF^-$ barely changed at all temperatures above 213 K (Fig. S39, ESI†), indicating that the two cationic guests underwent fast movement between the four corners, marking all twelve pyridyl units chemically equivalent. The addition of excess Na^+ into the solution of $(Na^+)_2\subset\star$ **T1**·$2BArF^-$ resulted in no further changes in the ^1H NMR spectrum, indicating that the accommodation of the third or more cations did not occur, due to coulombic repulsion.

The ability of **T1** to accommodate other alkali cations such as Li^+, K^+ and Cs^+ (Fig. S40–S59, ESI†), whose counterions are BF_4^-, $BArF^-$ and NTf_2^- respectively, was also investigated. The ^1H NMR spectroscopy results indicated that these cations exhibited similar host–guest recognition behaviors with the cage to Na^+. All the complexes underwent slow host–guest exchange on the timescale of ^1H NMR spectroscopy. As a consequence, the corresponding binding constants (K_1 and K_2) were measured by integrating the relevant resonances (Table 1). In $CDCl_3$, K_1 values for Na^+, K^+ and Cs^+ were measured to be

Table 1 The binding constants of the cage **T1** to recognize different cations

Cation	Anion	Solvent	K_1 (M^{-1})	K_2 (M^{-1})
Li^+	BF_4^-	$CDCl_3/CD_3CN$ (1 : 1 v/v)	$(1.9 \pm 0.2) \times 10^5$	$(2.3 \pm 0.1) \times 10^2$
Na^+	$BArF^-$	$CDCl_3$	$(1.1 \pm 0.02) \times 10^4$	$(1.7 \pm 0.5) \times 10^3$
Na^+	BF_4^-	$CDCl_3/CD_3CN$ (1 : 1 v/v)	$(2.7 \pm 0.2) \times 10^3$	Not bound
K^+	$BArF^-$	$CDCl_3$	$(3.0 \pm 0.8) \times 10^3$	$(7.3 \pm 0.3) \times 10^2$
K^+	BF_4^-	$CDCl_3/CD_3CN$ (1 : 1 v/v)	Not bound	Not bound
Cs^+	NTf_2^-	$CDCl_3$	$(2.9 \pm 0.3) \times 10^3$	$(4.4 \pm 0.1) \times 10^2$

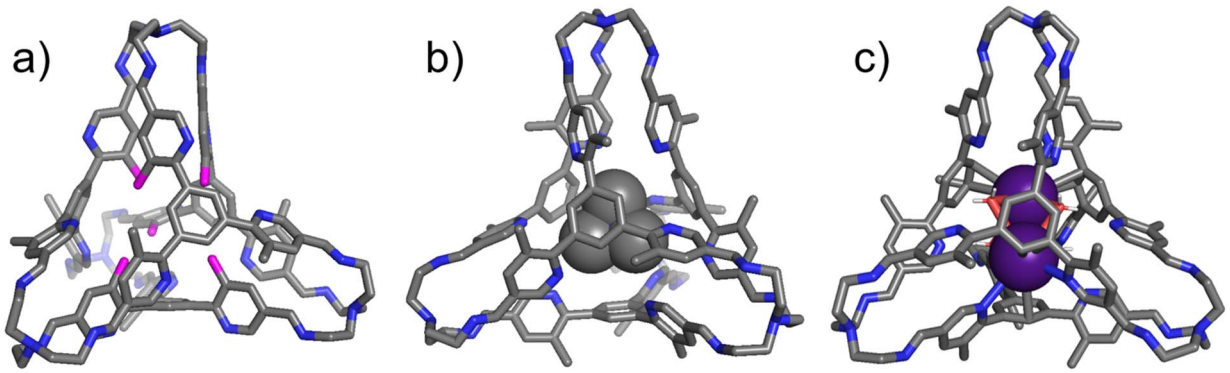

Fig. 4 Side views of the core structures of (a) **T1**, (b) $TMA^+ \subset$ **T1**$\cdot Cl^-$, and (c) $(Cs^+)_2 \subset$ **T1**$\cdot 2NTf_2^-$ from single crystal X-ray diffraction analysis. H white, C grey, N blue, O red, and Cs purple. Disordered solvent molecules, counterions namely Cl^- and NTf_2^- and hydrogen atoms which are not involved in hydrogen bonding interactions are omitted for the sake of clarity. In figure (a), there are six methyl units pointing inside the cage cavity, which were labelled with pink color.

$(1.09 \pm 0.02) \times 10^4\ M^{-1}$, $(2.96 \pm 0.76) \times 10^3\ M^{-1}$ and $(2.94 \pm 0.29) \times 10^3\ M^{-1}$, respectively, while K_2 values were measured to be $(1.73 \pm 0.47) \times 10^3\ M^{-1}$, $(7.3 \pm 0.3) \times 10^2\ M^{-1}$ and $(4.4 \pm 0.1) \times 10^2\ M^{-1}$, respectively. For all the cations, K_1 is larger than K_2 by nearly one order of magnitude, indicating that the binding of two cations within the cage cavity exhibits negative cooperativity. This observation is attributed to coulombic repulsion, which makes the accommodation of the second cation more energetically demanding. $Li^+ \cdot BF_4^-$ is poorly soluble in $CDCl_3$. We thus measured its K_1 and K_2 in a 1 : 1 mixture in $CDCl_3$ and CD_3CN, which are $(1.93 \pm 0.2) \times 10^5\ M^{-1}$ and $(2.3 \pm 0.1) \times 10^2\ M^{-1}$, respectively. We also performed binding experiments for Na^+ and K^+ in this mixture solvent (Fig. S60, ESI†). In the case of K^+, the cage exhibited little or no binding. In the case of Na^+, **T1** can only accommodate one equiv. of Na^+, even after the addition of an excess amount of Na^+ cation. K_1 of $Na^+ \subset$ **T1** was measured to be $(2.74 \pm 0.17) \times 10^3\ M^{-1}$ (Fig. S61, ESI†) in 1 : 1 $CDCl_3$ and CD_3CN, which is significantly lower than that in pure $CDCl_3$ by one order of magnitude. This observation indicated that the presence of CD_3CN suppressed the ability of the cage to accommodate cationic guests, probably because CD_3CN acts as a competitive ligand to coordinate with the cationic guests. In addition, smaller alkali cations such as Li^+ and Na^+ have larger binding affinity with the cage **T1** compared to their larger counterparts such as K^+ and Cs^+. This is not surprising, given that smaller cations have larger electron density and represent better Lewis acids. The ability of the cage to recognize transition metal cations such as Cu^+, Ag^+, Pd^{2+}, Zn^{2+} and Cd^{2+} and **T1** was also investigated (Fig. S95, ESI†). Unfortunately, the addition of these metal ions resulted in quick precipitation of cage, probably because of the formation of polymeric products on account of the coordination of the metal and pyridyl units in the cage framework.

Single crystals of the "free" cage **T1** (Fig. 4a), the complex $TMA^+ \subset$ **T1**$\cdot Cl^-$ (Fig. 4b), and the ternary complex $(Cs^+)_2 \subset$ ⋆ **T1**$\cdot 2NTf_2^-$ (Fig. 4c) were obtained by slow vapor diffusion of isopropyl ether into the corresponding solutions in chloroform. In the solid state structure of the "free" **T1**, six of its twelve methyl units reside inside the cage cavity and are labeled with pink color in Fig. 4a. Among these three methyl units, three are located in one corner and one resides in each of the other three corners. Close contacts were observed between the protons in these methyl units and either the adjacent pyridyl nitrogen atoms or the π-electron moieties, indicating the occurrence of either hydrogen bonding or CH···π interactions. In both $TMA^+ \subset$ **T1**$\cdot Cl^-$ and $(Cs^+)_2 \subset$ **T1**$\cdot 2NTf_2^-$, all twelve methyl units in the cage framework were observed to locate outside the cage cavity. As a consequence, all the pyridyl nitrogen atoms point inwards, forming either hydrogen bonds with the protons of TMA^+, or cation–dipole interactions with the Cs^+ cations. These results in solid state are consistent with the ^1H NMR spectroscopic results recorded in solution, namely that accommodating either a quaternary ammonium guest or two alkali cations drove all the methyl units to reside outside. The cavity of the cage in $(Cs^+)_2 \subset$ **T1**$\cdot 2NTf_2^-$ also encapsulates four water molecules. Each of the four water molecules forms one O–Cs bond with each of the two Cs^+ cations simultaneously. These water molecules act as glues between the two cationic guests, helping the latter suppress Coulombic repulsion. Attempts to obtain single crystals of the binary complexes such as $Na^+ \subset$ **T1**$\cdot BArF^-$ were unsuccessful.

Conclusions

To sum up, we successfully self-assembled a tetrahedral cage *via* imine condensation. The methyl units in the trisformyl building blocks play an important role in the cage formation, by introducing steric hindrance to afford a twisted conformation that favors the occurrence of intramolecular CH···π driving forces. Within the framework, each of the twelve *meta*-methylpyridyl units undergoes pivoting motion, affording the cage multiple conformations with a different number of methyl units pointing inwards/outwards. The "free" cage adopts a conformation where six methyl units point inward on average, as indicated by crystallography in solid state and ^1H NMR spectroscopy in solution. In the presence of a guest, the cage can switch its conformation to increase the effective volume of its cavity, by moving more methyl units outside and placing more

pyridyl nitrogen atoms inside. The latter units, which are Lewis basic binding sites, endow the cage with the ability to accommodate Lewis acidic guests. On average, after accommodating one alkali cation such as Na^+, nine of the twelve nitrogen atoms pointed inwards to form cation–dipole interactions with the guest. The effective volume of the cage cavity can be further increased, by adopting a conformation in which all twelve nitrogen atoms point inwards. This conformation allows the cage to accommodate either one quaternary ammonium guest or two alkali cations simultaneously. This cage modulating its conformation to optimize guest binding improves our understanding of the mechanism of how biological hosts employ allosteric effects to accomplish a variety of tasks, such as cargo loading and release within cells.

Data availability

The data supporting this article have been included as part of the ESI.† The X-ray crystallographic coordinates for structures reported in this study have been deposited at the Cambridge Crystallographic Data Centre (CCDC), under deposition numbers 2395426, 2441591 and 2396911. These data can be obtained free of charge from The Cambridge Crystallographic Data Centre *via* **https://www.ccdc.cam.ac.uk/structures**.

Author contributions

H. L. and H. T. conceived the concept. H. T. and Y. L. performed the experiments and analyzed the data. Y. Q. offered a variety of alkali cations. J. L. tested and refined the single crystals. H. C. provided beautiful image models. The manuscript was written through contributions of all authors. All authors have given approval to the final version of the manuscript.

Conflicts of interest

There are no conflicts to declare.

Acknowledgements

The research at Zhejiang University was supported by the Starry Night Science Fund of Zhejiang University Shanghai Institute for Advanced Study (No. SN-ZJU-SIAS-006). H. L. also wants to acknowledge the support from the Leading Innovation Team grant from the Department of Science and Technology of Zhejiang Province (2022R01005), the Natural Science Foundation of Zhejiang Province (No. LZ24B020002) and the National Natural Science Foundation of China (Grant No. 22471240). We thank Prof. Qiaohong He, Dr Jiyong Liu, Dr Yaqin Liu, Dr Lina Gao and Dr Yifan Zhao from the Chemistry Instrumentation Center at Zhejiang University for the technical support. We also thank Xiangqi Shao from the ZJU-Hangzhou Global Scientific and Technological Innovation Center for the VT NMR measurements.

Notes and references

1 D. Ringe and G. A. Petsko, How enzymes work, *Science*, 2008, **320**, 1428–1429.
2 G. K. Ackers, M. L. Doyle, D. Myers and M. A. Daugherty, Molecular code for cooperativity in hemoglobin, *Science*, 1992, **255**, 54–63.
3 F. J. Rizzuto, L. K. S. von Krbek and J. R. Nitschke, Strategies for binding multiple guests in metal-organic cages, *Nat. Rev. Chem.*, 2019, **3**, 204–222.
4 A. M. Lifschitz, M. S. Rosen, C. M. McGuirk and C. A. Mirkin, Allosteric Supramolecular Coordination Constructs, *J. Am. Chem. Soc.*, 2015, **137**, 7252–7261.
5 V. Marcos, A. J. Stephens, J. Jaramillo-Garcia, A. L. Nussbaumer, S. L. Woltering, A. Valero, J.-F. Lemonnier, I. J. Vitorica-Yrezabal and D. A. Leigh, Allosteric initiation and regulation of catalysis with a molecular knot, *Science*, 2016, **352**, 1555–1559.
6 I. A. Riddell, M. M. J. Smulders, J. K. Clegg, Y. R. Hristova, B. Breiner, J. D. Thoburn and J. R. Nitschke, Anion-induced reconstitution of a self-assembling system to express a chloride-binding $Co_{10}L_{15}$ pentagonal prism, *Nat. Chem.*, 2012, **4**, 860.
7 X. Li, J. Wu, L. Chen, X. Zhong, C. He, R. Zhang and C. Duan, Engineering an iridium-containing metal-organic molecular capsule for induced-fit geometrical conversion and dual catalysis, *Chem. Commun.*, 2016, **52**, 9628–9631.
8 C. M. Hong, D. M. Kaphan, R. G. Bergman, K. N. Raymond and F. D. Toste, Conformational Selection as the Mechanism of Guest Binding in a Flexible Supramolecular Host, *J. Am. Chem. Soc.*, 2017, **139**, 8013–8021.
9 D.-N. Yan, L.-X. Cai, P.-M. Cheng, S.-J. Hu, L.-P. Zhou and Q.-F. Sun, Photooxidase Mimicking with Adaptive Coordination Molecular Capsules, *J. Am. Chem. Soc.*, 2021, **143**, 16087–16094.
10 H. Liu, C. Guo, L. Li, Z. Zhang, Y. Hou, C. Mu, G.-l. Hou, Z. Zhang, H. Wang, X. Li and M. Zhang, Multicomponent, Multicavity Metallacages That Contain Different Binding Sites for Allosteric Recognition, *J. Am. Chem. Soc.*, 2024, **146**, 15787–15795.
11 K. Iizuka, H. Takezawa and M. Fujita, Template and Solid-State-Assisted Assembly of an M_9L_6 Expanded Coordination Cage for Medium-Sized Molecule Encapsulation, *J. Am. Chem. Soc.*, 2024, **146**, 32311–32316.
12 H. Xu, T. K. Ronson, A. W. Heard, P. C. P. Teeuwen, L. Schneider, P. Pracht, J. D. Thoburn, D. J. Wales and J. R. Nitschke, A pseudo-cubic metal-organic cage with conformationally switchable faces for dynamically adaptive guest encapsulation, *Nat. Chem.*, 2025, **17**, 289–296.
13 J. D. Crowley, A. J. Goshe and B. Bosnich, Molecular recognition. Self-assembly of molecular trigonal prisms and their host-guest adducts, *Chem. Commun.*, 2003, 2824–2825.
14 H. Sato, K. Tashiro, H. Shinmori, A. Osuka, Y. Murata, K. Komatsu and T. Aida, Positive heterotropic cooperativity for selective guest binding via electronic communications

through a fused zinc porphyrin array, *J. Am. Chem. Soc.*, 2005, **127**, 13086–13087.

15 J. D. Crowley, I. M. Steele and B. Bosnich, Molecular recognition - Allosterism generated by weak host-guest interactions in molecular rectangles, *Eur. J. Inorg. Chem.*, 2005, 3907–3917.

16 F. J. Rizzuto and J. R. Nitschke, Stereochemical plasticity modulates cooperative binding in a $Co^{II}_{12}L_6$ cuboctahedron, *Nat. Chem.*, 2017, **9**, 903–908.

17 N. J. Cookson, J. J. Henkelis, R. J. Ansell, C. W. G. Fishwick, M. J. Hardie and J. Fisher, Encapsulation of sodium alkyl sulfates by the cyclotriveratrylene-based, $[Pd_6L_8]^{12+}$ stella octangula cage, *Dalton Trans.*, 2014, **43**, 5657–5661.

18 W.-B. Hu, W.-J. Hu, Y. A. Liu, J.-S. Li, B. Jiang and K. Wen, Negative Cooperativity in the Binding of lmidazolium and Viologen Ions to a Pillar[5]arene-Crown Ether Fused Host, *Org. Lett.*, 2015, **17**, 2940–2943.

19 E. N. W. Howe, M. Bhadbhade and P. Thordarson, Cooperativity and Complexity in the Binding of Anions and Cations to a Tetratopic Ion-Pair Host, *J. Am. Chem. Soc.*, 2014, **136**, 7505–7516.

20 E. Lee, H. Ju, I.-H. Park, J. H. Jung, M. Ikeda, S. Kuwahara, Y. Habata and S. S. Lee, *pseudo*[1]Catenane-Type Pillar[5] thiacrown Whose Planar Chiral Inversion is Triggered by Metal Cation and Controlled by Anion, *J. Am. Chem. Soc.*, 2018, **140**, 9669–9677.

21 X. Wang, F. Jia, L.-P. Yang, H. Zhou and W. Jiang, Conformationally adaptive macrocycles with flipping aromatic sidewalls, *Chem. Soc. Rev.*, 2020, **49**, 4176–4188.

22 H. Guo, L.-W. Zhang, H. Zhou, W. Meng, Y.-F. Ao, D.-X. Wang and Q.-Q. Wang, Substrate-Induced Dimerization Assembly of Chiral Macrocycle Catalysts toward Cooperative Asymmetric Catalysis, *Angew. Chem., Int. Ed.*, 2020, **59**, 2623–2627.

23 D. Shimoyama, R. Sekiya, S. Inoue, N. Hisano, S.-I. Tate and T. Haino, Conformation Regulation of Trisresorcinarene Directed by Cavity Solvation, *Chem.–Eur. J.*, 2024, **30**, e202402922.

24 K.-D. Zhang, D. Ajami and J. Rebek, Hydrogen-Bonded Capsules in Water, *J. Am. Chem. Soc.*, 2013, **135**, 18064–18066.

25 B. P. Benke, T. Kirschbaum, J. Graf, J. H. Gross and M. Mastalerz, Dimeric and trimeric catenation of giant chiral [8 + 12] imine cubes driven by weak supramolecular interactions, *Nat. Chem.*, 2022, **15**, 413–423.

26 P. Skowronek and J. Gawronski, Chiral Iminospherand of a Tetrahedral Symmetry Spontaneously Assembled in a [6+4] Cyclocondensation, *Org. Lett.*, 2008, **10**, 4755–4758.

27 G. Zhang, O. Presly, F. White, I. M. Oppel and M. Mastalerz, A Permanent Mesoporous Organic Cage with an Exceptionally High Surface Area, *Angew. Chem., Int. Ed.*, 2014, **53**, 1516–1520.

28 M. Rondelli, A. H. Daranas and T. Martin, Importance of Precursor Adaptability in the Assembly of Molecular Organic Cages, *J. Org. Chem.*, 2023, **88**, 2113–2121.

29 S. Hollstein, O. Shyshov, M. Hanzevacki, J. Zhao, T. Rudolf, C. M. Jaeger and M. von Delius, Dynamic Covalent Self-Assembly of Chloride- and Ion-Pair-Templated Cryptates, *Angew. Chem., Int. Ed.*, 2022, **61**, e202201831.

30 A. D. Herrera-Espalia, H. Hopfl and H. Morales-Rojas, Host-Guest Properties of a Trigonal Iminoboronate Ester Cage Self-Assembled from Hexahydroxytriphenylene, *Eur. J. Org Chem.*, 2022, **2022**, e202200383.

31 L. Miton, E. Antonetti, D. Garcia-Lopez, P. Nava, V. Robert, M. Albalat, N. Vanthuyne, A. Martinez and Y. Cotelle, A Cyclotriveratrylene Solvent-Dependent Chiral Switch, *Chem.–Eur. J.*, 2024, **30**, e202303294.

32 H. Loew, E. Mena-Osteritz, K. M. Mullen, C. M. Jager and M. von Delius, Self-Assembly, Adaptive Response, and *in,out*-Stereoisomerism of Large Orthoformate Cryptands, *ChemPlusChem*, 2020, **85**, 1008–1012.

33 T. Jiao, L. Chen, D. Yang, X. Li, G. Wu, P. Zeng, A. Zhou, Q. Yin, Y. Pan, B. Wu, X. Hong, X. Kong, V. M. Lynch, J. L. Sessler and H. Li, Trapping White Phosphorus within a Purely Organic Molecular Container Produced by Imine Condensation, *Angew. Chem., Int. Ed.*, 2017, **56**, 14545–14550.

34 T. Jiao, G. Wu, L. Chen, C.-Y. Wang and H. Li, Precursor Control over the Self-Assembly of Organic Cages via Imine Condensation, *J. Org. Chem.*, 2018, **83**, 12404–12410.

35 T. Jiao, H. Qu, L. Tong, X. Cao and H. Li, A Self-Assembled Homochiral Radical Cage with Paramagnetic Behaviors, *Angew. Chem., Int. Ed.*, 2021, **60**, 9852–9858.

36 Y. Chen, G. Wu, B. Chen, H. Qu, T. Jiao, Y. Li, C. Ge, C. Zhang, L. Liang, X. Zeng, X. Cao, Q. Wang and H. Li, Self-Assembly of a Purely Covalent Cage with Homochirality by Imine Formation in Water, *Angew. Chem., Int. Ed.*, 2021, **60**, 18815–18820.